

Facile eco-friendly treatment of a dye wastewater mixture by *in situ* hybridization with growing calcium carbonate†

Dan-Hua Zhao, Ya-Lei Zhang, Yan-Ping Wei and Hong-Wen Gao*

Received 17th June 2009, Accepted 3rd August 2009

First published as an Advance Article on the web 24th August 2009

DOI: 10.1039/b911830f

Inorganic/organic hybridization is often employed to synthesize functional materials but seldom considered in industrial wastewater treatment. Dye conjugate hybridization was proposed by immobilizing the anionic (*e.g.* congo red)–cationic (*e.g.* methylene blue) dye complex with growing calcium carbonate. The 3D-morphology and structure of the conjugate hybrid were characterized and the mechanism of formation elucidated. The shell–core structural hybrid was formed and then stacked into cubes. Applied to treatment of concentrated organic wastewaters, the simple single-step hybridization performed adsorption, flocculation and ionic complexation and exhibited a high level of removal of organic substances. This work provides a convenient, cost-effective and environment-friendly wastewater treatment by “using waste to treat waste”.

Introduction

Nowadays, over 10,000 dyes are commercially available and more than 700,000 tonnes are produced annually. The colored effluents discharged from textile processing and dye-manufacturing industries contain a significant amount of unreacted dye. During dyeing processes, up to 15% of the dyestuff doesn't bind to the fibers and is therefore released into the environment.¹ Azo dyes, being the largest group of synthetic dyes, constitute up to 70% of all the known commercial dyes produced.² Their chemical structures are often characterized by highly substituted aromatic rings joined by one or more azo groups (–N=N–). They lead to acute toxic effects on the flora and fauna of the ecosystem when released into the environment. Moreover, many azo dyes and their metabolites are mutagenic and carcinogenic.³ The majority of color removal techniques are based on coagulation/adsorption of dyes by physical methods or the complete destruction of dye molecules by chemical methods such as electrolysis, ozonation, *etc.* Treatment of textile wastewater in Europe mostly occurs in conventional municipal wastewater treatment systems.⁴ However, the conventional treatments have inherent drawbacks as they generate a significant amount of sludge or cause secondary pollution due to formation of hazardous by-products.⁵ Though the combination of physical and biological treatments achieves a satisfactory removal of organic contaminants,⁶ the complicated procedure and long period brought out a high running cost and secondary pollution. Thus, highly concentrated wastewater treatment must focus on innovative methods together with the recycling of waste.

As is well known, inorganic-organic hybridization is often employed in the synthesis of functional materials (*e.g.* photo-sensitive cells, optical thin films and sensors)⁷ but seldom

considered for water pollution control, *e.g.* industrial wastewater treatment. The objective of this work is to establish a new type of wastewater treatment method by immobilizing waste anionic (*e.g.* congo red, CR)–cationic (*e.g.* methylene blue, MB) dyes by conjugation onto a harmless inorganic skeleton (*e.g.* CaCO₃) (Fig. 1A–C). Also, based on the dye wastewater characteristics, the feasibility of reuse of the dye-immobilized CaCO₃ sludge was investigated (*e.g.* as filler in polymer products) in order to avoid secondary pollution (Fig. 1D–E).

Experimental section

Apparatus and materials

A photodiode array spectrometer (Model S4100, Scinco, Korea) with the Labpro plus software (Firmware Version 060105) was used to determine chromaticity and concentration of various color compounds and suspended substance liquids. A particle size analyzer (Model LS230, Beckman Coulter, USA) with a Laser Channel (Model LFC-101, Ankersmid, Holland) was used to measure the size distribution and specific surface area (SSA) of the material particles. An X-ray diffractometer (XRD) (Model D/max 2550VB3+/PC, Rigaku, Japan) was used for identifying the structure and size of crystal particles. Scanning electronic microscopy (SEM) (Model Quanta 200 FEG, FEI Co., USA) was used to measure the size and shape of the materials. High resolution transmission electronic microscopy (TEM) (Model Tecnai G2 F20 S-Twin, FEI Co., USA) (120 kV, 2.4 Å resolution) was used to measure the distribution of CaCO₃, CR and MB in the particle fragments. Infrared (IR) spectra of the hybrid in KBr pellet were obtained, using an infrared spectrometer system (Model Equinox/hyperion 2000, BRUKER Co., Germany). A programmable digestion system (Model 5B-1, Lanzhou, China) and a portable chemical oxygen demand (COD) analyzer (Model PORS-15V, Pgeneral Co., China) were coupled for determination of COD in wastewater.

The following dye solutions were prepared by dissolving in distilled water: CR (C.I. 22120), MB (C.I. 52015), weak acidic

State Key Laboratory of Pollution Control and Resource Reuse, College of Environmental Science and Engineering, Tongji University, Shanghai, 200092, China. E-mail: hwgao@tongji.edu.cn; Fax: (+)86-21-65988598

† Electronic supplementary information (ESI) available: Fig. S1–S8. See DOI: 10.1039/b911830f

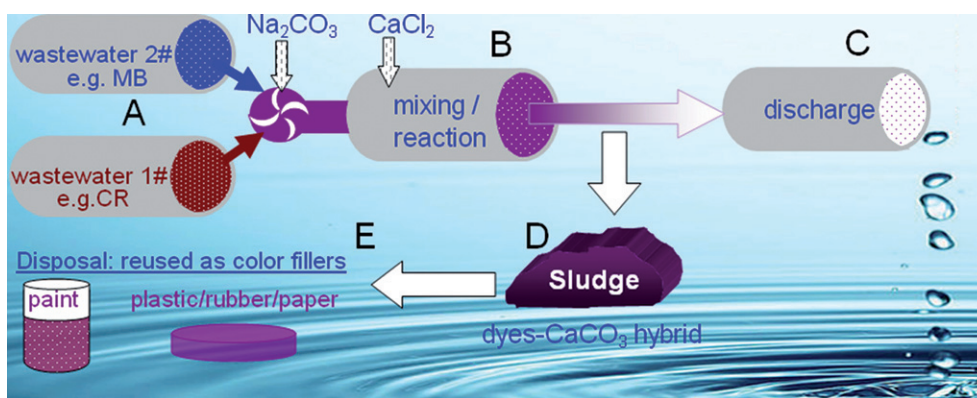


Fig. 1 Cartoon illustration of the two-dye (CR/MB) mixture treatment process. A: CR mixed with MB; B: Na_2CO_3 and then CaCl_2 were added. The treatment water was discharged after settling the suspending substance (C) and the dye-contaminated sludge separated (D). The colored sludge was reused as the color filler of a polymer product (E).

green GS (C.I. 61580), methylene violet (C.I. 52041), basic brilliant blue BO (C.I. 42595), cationic red 3R (C.I. 48013), reactive brilliant red K-2BP (C.I. 18208), reactive brilliant red X-3B (C.I. 18200) and acid brilliant blue 6B (C.I. 42660). Both PVC and di-n-octyl phthalate (DOP) in A. R. grade were purchased from Shanghai Reagents and Shanghai Hengda Fine Chemicals, China. Two dye wastewaters (1# and 2#, unknown cationic dyes) were sampled from Jinjiang Chemicals (Hangzhou, China) and Xingwu Dye Plant (Nantong, China), respectively. Their color strengths were determined to be 27,000 (1# - blue) and 15,000 (2# - red) by spectrophotometry and their CODs to be 870 (1#) and 710 mg/L (2#) by COD analyzer. CR wastewater (1.8 mM) was prepared with a river water as the anionic dye wastewater.

Methods

Formation and characterization of the dye conjugate- CaCO_3 hybrid. The anionic dye, CR (2.0 mM) was mixed with a cationic dye e.g. MB (4.0 mM) and sodium carbonate (0.02 M) was added. After mixed thoroughly, calcium chloride (0.04 M) was added slowly under stirring. After 30 min, the suspending substance product was precipitated and washed with deionized water. Finally, approximately 10% product aqueous liquid was prepared with deionized water and it aged for 48 h. The particle size distribution was measured, and TEM and SEM were performed on the suspended substance and the dried powder used for the XRD and IR measurement.

In situ treatment of organic wastewater. The CR wastewater (1.8 mM) was mixed with a cationic wastewater. Sodium carbonate (0.06 M) was added. After mixing for 5 min, calcium chloride (0.12 M) was added in the ratio of 2 : 1 of the constant molar ratio of Ca^{2+} : CO_3^{2-} . The liquid was mixed thoroughly. After 30 min, the color strength of supernatant was determined by spectrophotometry and COD with a COD analyzer. Thus, the decolorization rate of dye wastewater and the removal of COD were calculated.

Disposal of dye-contaminated sludge reused as color filler. The CR-MB conjugate- CaCO_3 sludge formed above was dried for

3 h at 120 °C and then milled into a fine powder after cooling to room temperature. 0.1 g of the powder was mixed together with 0.1 g of PVC. The mixture was put into a cylindrical glass bottle and 7.0 g of DOP added. After mixing thoroughly, it was dried for 1.5 h at 150 °C. After cooling, the shaped cylindrical colored plastic was immersed in neutral aqueous media (pH 6.5) and 0.1 M NaOH (pH 13) for 24 h, respectively, where all the media were 100 ml in volume. The release of colored substances was observed. According the above method, a reference plastic was prepared and the CR-MB mixture immersed in it (0.02 g in 2 moles of the ratio of MB to CR) instead of the sludge powder.

Results and discussion

Structure and pattern of the dye conjugate- CaCO_3 hybrid

The optimization indicated that, Ca^{2+} being double the CO_3^{2-} molarity and CO_3^{2-} over 10 times higher, CR caused the rapid sedimentation of dyes with growing CaCO_3 (refer to ESI,† Fig. S1). The optimal addition sequence of the reactants is CR, MB, CO_3^{2-} and then Ca^{2+} .⁸ The CaCO_3 crystal particles are rectangular prisms (Fig. 2A). The surface is smooth and the edges and angles sharp and clear. Many rectangular prisms

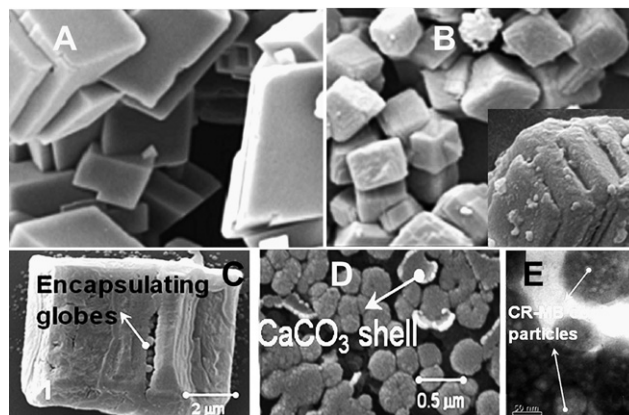


Fig. 2 SEM images of CaCO_3 -only (A) and CR-MB conjugate- CaCO_3 hybrid materials (B), after aging and during the middle growth procedure (C). TEM (D) and SEM (E) images of the stacking particles.

aggregate and wedge each other together. However, the CR–MB conjugate–CaCO₃ hybrid (Fig. 1D) changed into smaller cubes (Fig. 2B) stacking layer-on-layer. Different to CaCO₃-only crystal particles, the dye complex hybrid particles have rough surface with cambered edges and corners. From the SEM images of growing CR–MB conjugate–CaCO₃ particles, various rectangular encapsulation bags were filled with lots of globes in size between 50 and 100 nm (Fig. 2C, refer to ESI,† Fig. S2 B, C, E) and these nanoglobes are the core–shell structures (Fig. 2D, refer to ESI,† Fig. S2G). The immobilization of the conjugate inhibited the self-stacking of CaCO₃ and also the particles became smaller than CaCO₃-only ones (refer to ESI,† Fig. S3). By comparison of the XRD results (refer to ESI,† Fig. S4), it was shown that no other crystal structures were formed except for CaCO₃ crystals. Furthermore, the presence of the CR–MB conjugate made the hybrid particles smaller. The CR–MB conjugate aggregated into lots of sticky nanosized globes (refer to ESI,† Fig. S2D) to form a core (Fig. 2E) being obviously different from the single dye hybrid.^{8b} The immobilization of organic substances was confirmed from the bright diffraction spots (refer to ESI,† Fig. S2H) and CaCO₃ grew outside to form a shell, confirmed by the Ca : S ratio of between 15 and 30 (refer to ESI,† Fig. S2I). From the addition sequence of the reactants, the nanosized CR–MB conjugate particles had formed before the CaCO₃ growth. By comparing the water-washing effect of the CR–MB conjugate–CaCO₃ hybrid with that of the CaCO₃ surface-modifying CR–MB complex (refer to ESI,† Fig. S5), the dyes in the CaCO₃ hybrid were seldom released into the aqueous phase. Furthermore, the hybrid settled down within 30 min. On the contrary, an obvious dissolution of dyes occurred in the surface-modifying material liquid. Without doubt, both CR and MB in the CaCO₃ hybrid couldn't have been adsorbed on the outside surface of the hybrid particles.

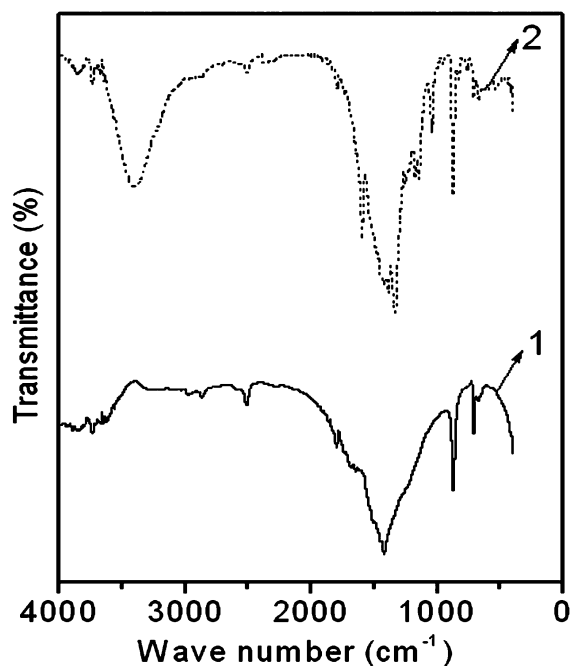


Fig. 3 IR spectra of CaCO₃ (1) and the CR–MB conjugate –CaCO₃ hybrid (2).

The IR spectrum (Fig. 3) revealed the difference in composition between the CaCO₃-only and the CR–MB conjugate –CaCO₃ hybrid. It is well-known that CaCO₃ has characteristic vibration bands, such as Ca–O stretching and bending vibrations, and stretching vibrations (CO₃²⁻). A set of strong and wide peaks nearby 1430 cm⁻¹ from curve 1 can be assigned to the $\nu(\text{CO}_3^{2-})$ stretching vibration band for CaCO₃, while the middle strong peak at 877 cm⁻¹ and small peak at 715 cm⁻¹ are the characteristic bending and rocking vibration bands of CO₃²⁻ and Ca–O stretching and bending vibrations,⁹ respectively. Compared to unmodified CaCO₃, curve 2 shows the IR spectrum of the CR–MB conjugate–CaCO₃ hybrid was more complicated. The IR band at 3430 cm⁻¹ of hybrid nano-CaCO₃ is intense, which is attributable to N–H stretching vibrations for CR combining with MB in CaCO₃. In addition, the $\nu(\text{SO}_3^-)$ peak at 1050 cm⁻¹ demonstrated the electrostatic interaction of =N⁺ with –SO₃⁻. From curve 2, the IR band from 1300 to 1550 cm⁻¹ and the more intense characteristic bending and rocking vibration peak of CO₃²⁻ at 880 cm⁻¹ can be assigned to characteristic IR absorption because of the mutual influence of aromatic characteristics adsorption peaks in CR and MB at 1600–1430 cm⁻¹, the N=N adsorption peak near 1500 cm⁻¹ and the $\nu(\text{CO}_3^{2-})$ stretching vibration band, which is convincing evidence of the CR–MB conjugate hybridized with the growing calcium carbonate. Moreover, the vibration peak at 1321 cm⁻¹ of =C–H; 1600 cm⁻¹ of C=N; 1180 cm⁻¹ of C–N in MB and CR were found.¹⁰

From the above analyses, the formation mechanism of the CR–MB conjugate –CaCO₃ hybrid is illustrated in Fig. 4. The CR–MB mixture may form the nanosized aggregate globe *via* ion pair complexation (1). Lots of Ca²⁺ bound to the globe surface *via* affiliation with –SO₃⁻ of CR (2) and then CO₃²⁻ reacted with the Ca²⁺ on the globe surface to form the CaCO₃ outside shell (3, 4). Lots of the CR–MB–CaCO₃ particles stacked into the encapsulation bags and then the laminar cube after aging (5) (Fig. 2 B).

Adsorption selectivity

Besides MB (Fig. 5A), the other three cationic dyes (tubes labelled 1): methylene violet (B), basic brilliant blue BO (C) and cationic red 3R (D) and four anionic dyes (tubes labelled 1): weak acidic green GS (E), acidic brilliant blue 6B (F), reactive brilliant red X-3B (G) and reactive brilliant red K-2BP (H) were mixed with CR (tubes labelled 2) and immobilized with growing CaCO₃ (tubes labelled 3), approximately 0.06%, *i.e.* 6 mM Na₂CO₃

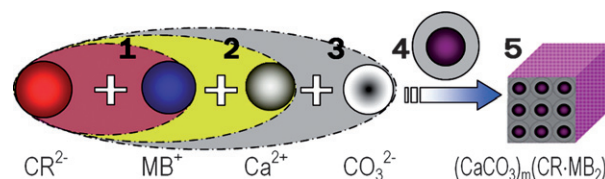


Fig. 4 A schematic diagram of the formation process of the CR–MB conjugate–CaCO₃ hybrid material. 1: CR–MB mixed to form a complex; 2: the CR–MB complex attracted Ca²⁺; 3: aggregation of CO₃²⁻ on the CR–MB–Ca²⁺ surface; 4: CR–MB core with CaCO₃ shell; 5: the CR–MB conjugate–CaCO₃ hybrid material formed after aging.

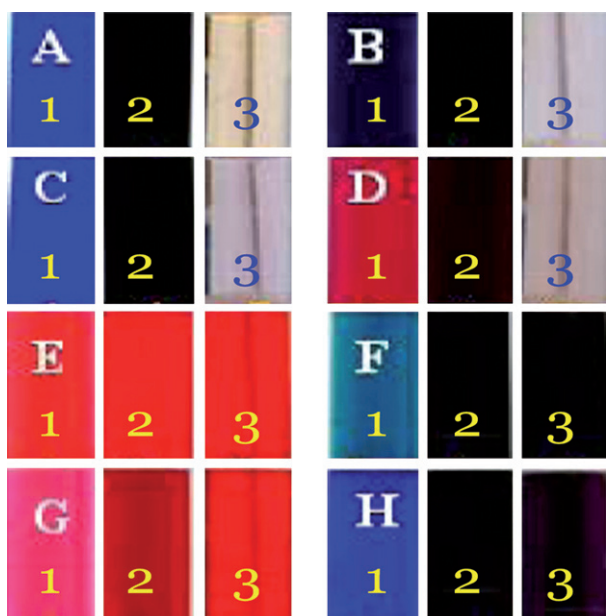


Fig. 5 Photos illustrating color change of dye supernatants: MB (A), methylene violet (B), basic brilliant blue BO (C), cationic red 3R (D), reactive brilliant red K-2BP (E), weak acid green GS (F), reactive brilliant red X-3B (G) and acid brilliant blue 6B (H). All dyes are in 200 μM . 1: dye-only; 2: dye mixed with 200 μM CR; 3: dye-CR mixture treated by adding 10.0 mM CO_3^{2-} and 20.0 mM Ca^{2+} . All liquids were settled for 30 min.

mixed with 12 mM CaCl_2 . The color strength of all anionic dye supernatants hasn't obviously change by comparison of tube 3 with tube 2 (E and H). It indicates that a mixture of two anionic dyes cannot form a conjugate complex but a little of them may be immobilized independently onto growing CaCO_3 by comparison of tube 3 with tube 2 (G and H). From the tubes labelled 3 (A–D), all the CR cationic dye mixtures become almost colorless when treated with growing CaCO_3 . The cationic dyes all complex with CR and their conjugates were hybridized readily with growing CaCO_3 then removed. As a result, ion-pair complexation is the major interaction between cationic and anionic dyes.

Effect of dye concentration

From the curve in Fig. 6, the equilibrium concentration of MB remains at 0 when MB is less than double the CR molarity. The amount of free MB began to increase rapidly when the initial concentration of MB is over 400 μM . Without doubt, two MB molecules bound to one CR molecule and they formed a 2 : 1 complex as illustrated in Fig. 6. With the same method, the other three cationic dyes: methylene violet, basic brilliant blue BO and cationic red 3R also gave the same result. Thus, ion-pair interaction occurred between CR and a cationic dye. Without doubt, the optimal concentration ratio of two dyes depend on ion pair equilibrium (refer to ESI,† Fig. S6).

Effect of CaCO_3 on the sedimentation rate

Various addition concentrations of CO_3^{2-} and Ca^{2+} affected the sedimentation rate of the conjugate hybrid (Fig. 7). The presence of growing CaCO_3 accelerated obviously the sedimentation of

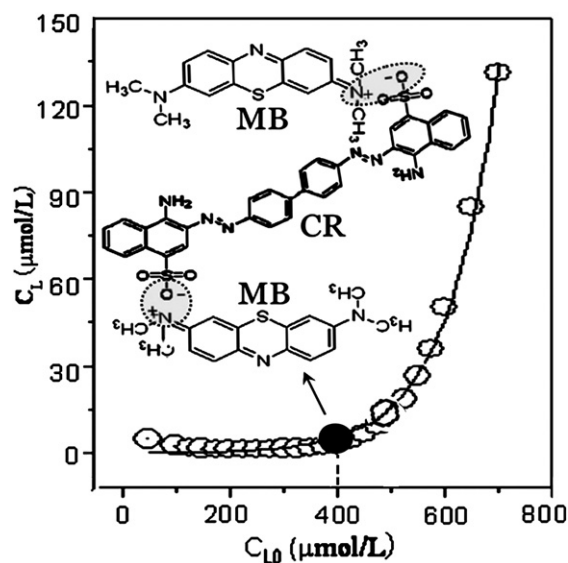


Fig. 6 Change of MB equilibrium concentration (c_1) with its initial concentration (c_{L0}). All the solutions contained 200 μM CR and were treated with growing CaCO_3 (0.06%). The $\text{CR}(\text{MB})_2$ complex was formed at 1 : 2 of the mole ratio of CR to MB and its structure is illustrated.

the conjugate hybrid, specially within 20 min. The increases of CO_3^{2-} and Ca^{2+} concentration is favorable for the sedimentation of the conjugate hybrid. The hybrid settled down from 8 cm of thickness to only 1.8 cm within 30 min (refer to ESI,† Fig. S1) when CO_3^{2-} is more than 0.02 M, *i.e.* 10 of the mole ratio of CaCO_3 to CR.

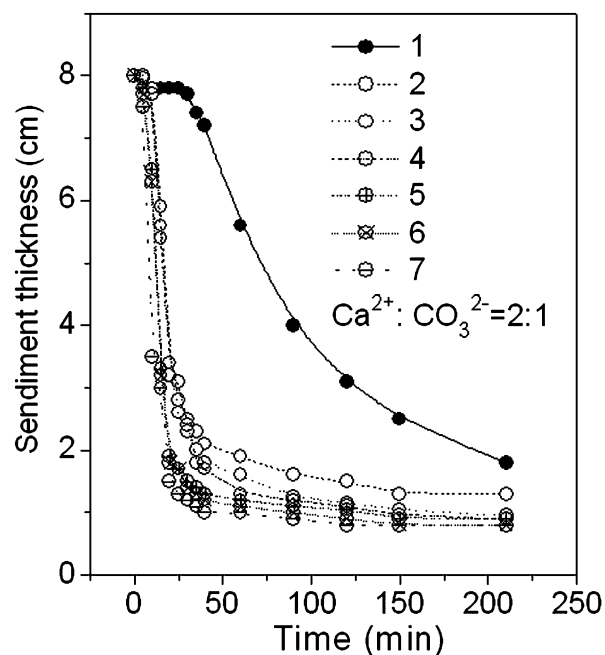


Fig. 7 Variation of the sedimentation rate of the CR (2.0 mM)–MB (4.0 mM) conjugate – CaCO_3 hybrid when treated by adding various CO_3^{2-} and Ca^{2+} concentrations at the constant mole ratio –2 of Ca^{2+} to CO_3^{2-} . From 1 to 7: 0.01, 0.02, 0.05, 0.08, 0.10, 0.12 and 0.15 M CO_3^{2-} .

Effects of pH, electrolyte and temperature

Effect of pH indicated that on removal of the CR–MB mixture color strength remained high when treated with growing CaCO_3 at $\text{pH} > 3$. This is attributed to the fact that CaCO_3 would be dissolved in a strong acidic medium. The presence of concentrated electrolyte is favorable for the salting-out of the CR–MB conjugate. However, no obvious sediment appeared in 30 min when electrolyte concentration was less than 0.1 M. The temperature has little effect for the *in situ* coprecipitation of the CR–MB conjugate (refer to ESI,† Fig. S7).

Comparison of adsorption capacity

When a cationic dye was mixed with CR according to ion-pair equilibrium, a dye conjugate was formed and then precipitated rapidly together with CaCO_3 . Different from a conventional adsorbent, the *in situ* immobilization of the CR–MB conjugate in growing CaCO_3 has no direct correlation with the surface area of material. From the above experimental results, the adsorption capability of growing CaCO_3 was calculated to be 217 mg CR and 213 mg MB per gram CaCO_3 and also their adsorptions occurred simultaneously. From Table 1, the CR-sorbing capacity of the adsorbents *e.g.* activated carbon, fly ash and so on is between 3.0 and 66.23 mg/g and the MB-sorbing capacity between 4.92 and 27.78 mg/g.¹¹ Therefore, the dye conjugate hybridization resulted in a much more dye removal than those by using the conventional adsorbents.

In situ treatment of dye wastewater mixtures

Recycling and reuse of waste has been given increasing attention.¹² Two unknown cationic dye wastewaters (1# - blue and 2# - red) and a CR wastewater were mixed respectively and treated with growing CaCO_3 . The color strength of wastewater 1 decreased by 99.4% (Fig. 8A) and the removal of COD is over 83% (Fig. 8B) when only 0.01 M CO_3^{2-} and 0.02 M Ca^{2+} were added, *i.e.* approximately 0.1% CaCO_3 formed. The decolorization of wastewater 2 is 98.5% (Fig. 8A) and the removal of COD over 71% (Fig. 8B). The COD of wastewater 1 decreased to less than the limit of detection (LOD), *i.e.* 150 mg/L from 870 mg/L. Besides CR, some organic substances with sulfonic acid groups coexisting in wastewater may be immobilized onto the growing

Table 1 Adsorption capacity of various adsorbents for removals of MB and CR¹¹

Adsorbents	Dye	Adsorption capacity (mg/g)
growing CaCO_3	MB	213
	CR	217
saw dust-pitch pine	MB	27.78
coconut coir	MB	15.59
class fly ash	MB	4.92
fly ash- HNO_3	MB	7.74
activated carbon	MB	17.63
FA-C	CR	31.14
baggage fly ash	CR	11.84
activated carbon	CR	3.0
orange peel	CR	22.40
palm kernel seed coat	CR	66.23

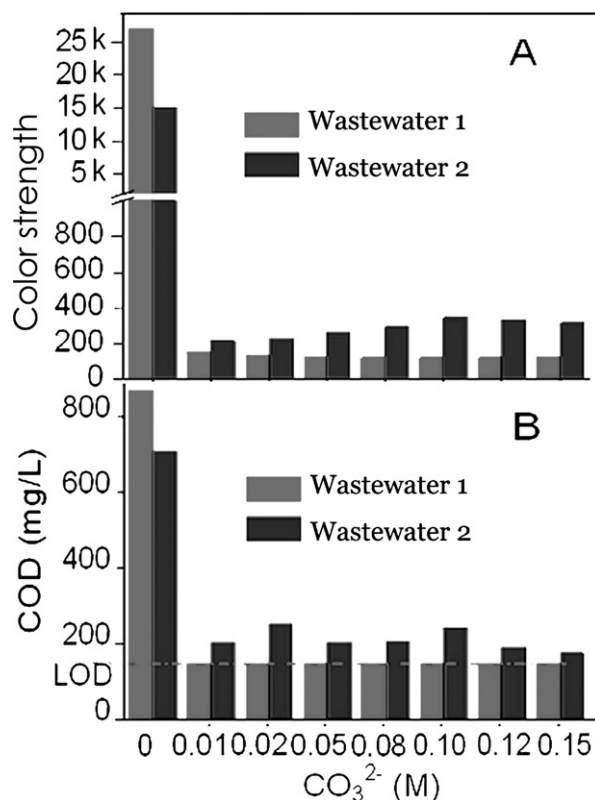


Fig. 8 Changes in color strength (A) and COD (B) in two kinds of dye wastewater sampled from: 1# - Jinjiang Chemicals and 2# - Xingwu Dye Plant when treated with CR wastewater (1.8 mM), Na_2CO_3 (from 0.01 to 0.15 M) and CaCl_2 (from 0.02 to 0.3 M).

CaCO_3 . After the sludge was separated, the treatment water can be discharged into an aquatic environment (Fig. 1C).

Disposal of dye-contaminated sludge

The fine powder of dye-contaminated sludge was tried as the color filler of polymer products *e.g.* plastic, paint and rubber (Fig. 1E). As an example, a colored plastic was prepared by adding the above sludge powder into the mixture of PVC and DOP and the cylindrical product was immersed in neutral and basic aqueous media. No color substance was released within 24 h (refer to ESI,† Fig. S8). On the contrary, for the CR–MB mixture adding plastic product caused an obvious color release. Beyond all doubt, using the dye– CaCO_3 hybrid sludge in the polymer product raised the fastness of color substance, *i.e.* resistance to weakly acidic to alkalic media. As is well known, calcium carbonate is often employed as the reinforcing filler during the production of paint, rubber, paper and plastic. Furthermore, such waste sludge disposal may prevent secondary contamination from happening. Consequently, the dye– CaCO_3 hybrid sludge reused as the color filler instead of both dye additive and calcium carbonate filler may achieve a double effect similar to “killing two birds with one stone”.

Conclusions

Dye conjugate hybridization was developed by immobilizing the CR–MB complex into growing CaCO_3 . The shell–core structural

dye conjugate-CaCO₃ hybrid was formed and they stacked together into cubes after aging. Such a hybridization simultaneously performed the adsorption, flocculation and ion pair complexation and the growing CaCO₃ exhibited a high adsorption capacity in pH > 3 aqueous media when simultaneously adsorbed cationic and anionic dyes. The simple one-step process has realized *in situ* treatment of two kinds of dye wastewaters with satisfactory removal of organic substances. Also, the dye-contaminated sludge is a potential color filler which can be feasibly reused in polymer products. This work developed a facile, practical and eco-friendly wastewater treatment method by “using waste to treat waste” and reusing waste.

Acknowledgements

We thank the National Key Technology R&D Program of China (Grant No. 2006BAJ08B10) and the National S&T Major Project of China (No.2008ZX07421-002) for financially supporting this work.

Notes and references

- 1 M. S. Khehra, H. S. Saini, D. K. Sharma, B. S. Chadha and S. S. Chimni, *Water Res.*, 2005, **39**, 5135–5141.
- 2 C. M. Carliell, S. J. Barclay, C. Shaw, A. D. Wheatley and C. A. Buckley, *Environ. Technol.*, 1998, **19**, 1133–1137.
- 3 K. T. Chung and C. E. Cerniglia, *Mutat. Res., Rev. Genet. Toxicol.*, 1992, **277**, 201–220.
- 4 C. T. M. J. Frijters, R. H. Vos, G. Scheffer and R. Mulder, *Water Res.*, 2006, **40**, 1249–1257.
- 5 P. Verma, P. Baldrian and F. Nerud, *Chemosphere*, 2003, **50**, 975–979.
- 6 M. S. Lucas, A. A. Dias, A. Sampaio, C. Amaral and J. A. Peresa, *Water Res.*, 2007, **41**, 1103–1109.
- 7 (a) S. Mintova, V. D. Waele, U. Schmidhammer, E. Riedle and T. Bein, *Angew. Chem., Int. Ed.*, 2003, **42**, 1611–1614; (b) Q. F. Zhang, T. P. Chou, B. Russo, S. A. Jenekhe and G. Z. Cao, *Angew. Chem., Int. Ed.*, 2008, **47**, 2402–2406; (c) J. H. Zhu, S. H. Yu, A. W. Xu and H. Cölfen, *Chem. Commun.*, 2009, 1106–1108; (d) J. Zhong and M. M. Maye, *Adv. Mater.*, 2001, **13**, 1507–1511; (e) H. P. Cong and S. H. Yu, *Adv. Funct. Mater.*, 2007, **17**, 1814–1820; (f) S. A. Haque, E. Palomares, H. Upadhyaya, L. Ottley, R. J. Potter, A. B. Holmes and J. R. Durrant, *Chem. Commun.*, 2003, 3008–3009; (g) Y. Takahashi, H. Kasai, H. Nakanishi and T. M. Suzuki, *Angew. Chem., Int. Ed.*, 2006, **45**, 913–916; (h) E. Palomares, R. Vilar and J. R. Durrant, *Chem. Commun.*, 2004, 362–363.
- 8 (a) H. Y. Wang and H. W. Gao, *Environ. Sci. Pollut. Res.*, 2009, **16**, 339–347; (b) J. Lin and H. W. Gao, *J. Mater. Chem.*, 2009, **19**, 3598–3601.
- 9 N. Kazuo, *Infrared Spectra of Inorganic and Coordination Compounds [M]*, Wiley & Sons, 4th edn, 1986, 156.
- 10 (a) Y. H. Chu, G. B. Zhang, Y. G. Zhao, S. Z. Yu, J. W. Wang and B. J. Li, *Spectrosc. Spect. Anal.*, 2007, **27**, 1510–1513; (b) Y. J. Tang, Y. M. Li and Z. H. Chen, *J. Shanxi Univ. Sci. Tech.*, 2007, **25**, 57–62.
- 11 (a) A. Aygun, S. Yenisooy-Karakas and I. Duman, *Microporous Mesoporous Mater.*, 2003, **66**, 189–195; (b) Y. C. Sharma, Uma and S. N. Upadhyay, *Energy Fuels*, 2009, **23**, 2983–2988; (c) S. Wang, Y. Boyjoo, A. Chouei and Z. H. Zhu, *Water Res.*, 2005, **39**, 129–138; (d) S. Karaca, A. Gürses, M. Acikyildiz and M. Ejder, *Microporous Mesoporous Mater.*, 2008, **115**, 376–386; (e) B. J. Acemioglu, *J. Colloid Interface Sci.*, 2004, **274**, 371–379; (f) I. D. Mall, V. C. Srivastava, N. K. Agarwal and I. M. Mishra, *Chemosphere*, 2005, **61**, 492–501; (g) M. K. Purkait, A. Maiti, S. Das Gupta and S. J. De, *J. Hazard. Mater.*, 2007, **145**, 287–295; (h) C. Namasivayam, N. Muniasamy, K. Gayatri, M. Rani and K. Ranga-nathan, *Bioresour. Technol.*, 1996, **57**, 37–43; (i) N. A. Oladoja and A. K. Akinlabi, *Ind. Eng. Chem. Res.*, 2009, **48**, 6188–6196.
- 12 (a) A. Tal, *Science*, 2006, **313**, 1081–1084; (b) W. Z. Liu, F. Huang, Y. Q. Liao, J. Zhang, G. Q. Ren, Z. Y. Zhuang, J. S. Zhen, Z. Liu and C. Wang, *Angew. Chem., Int. Ed.*, 2008, **47**, 5619–5622; (c) F. M. Jin, J. Yun, G. M. Li, A. Kishita, K. Tohji and H. Enomoto, *Green Chem.*, 2008, **10**, 612–615; (d) D. K. S. Ng, D. C. Y. Foo and R. R. Tan, *Ind. Eng. Chem. Res.*, 2007, **46**, 9107–9113.